



SAPIENZA
UNIVERSITÀ DI ROMA

EODA

HW 1: VEGETATION COVER FROM MODIS TERRA/AQUA DATA

Author:
Francesco Romeo

Supervisor:
Frank S. Marzano

August 2020

1 Download a first MODIS image at 1-km resolution over Italy or other geographical area of interest during a summer season from <https://ladsweb.modaps.eosdis.nasa.gov/search> (select MYD021KM*.*).

As first step, it has been necessary to download a product from the LAADS DAAC Nasa website. In order to do that a query has been performed on their database in order to return all the products matching the pulled request: the product has to be a MODIS image with 1 km resolution, level 1 data (meaning calibrated radiances data), covering the Italy country during the summer period in 2019. The selected product is the one reported below:

- **24 August 2019:** MYD021KM.A2019236.1220.006.2019238185820.hdf

By looking at the product file name, it is possible to see that is composed by 5 fields:

- **Product Short name:** MYD021KM, where *MYD* stands for Aqua platform, *02* stands for calibrated product, *1KM* is the spatial resolution
- **Julian Date of Acquisition:** A2019236, *A* stands for acquisition and *236* is the 236th day
- **Hours and Minutes of Acquisition:** 1220
- **Collection Version:** 006
- **Julian Date of Production:** 2019238185820
- **Data Format:** hdf

Terra and Aqua satellites, carrying MODIS instruments, are sun-synchronous, near-polar, circular orbit. They provide product data in 36 spectral bands spanning from 0.4 μm to 14.4 μm . The Swath has a cross track of 2330 km whereas an along track at nadir of 10 km.

2 Perform data quality check

Once the product has been downloaded and opened in SNAP, what is always recommended to do is to take a look at the product in order to understand what it contains. The product is composed by 4 sections. The first one is the **Metadata** containing general information about the product that can be used to check its quality. Figure 1 shows what are the general_attributes of the product. As can be seen from the Figure, the image has been taken after 203 scans all performed during daylight. It also tells that no incomplete scans occurred. Moreover, it tells that the product is a SWATH product and that the time between the starting SWATH and the end SWATH is of roughly 5 minutes. It actually contains also some redundant information, in the sense that it also reports the spatial resolution and the MODIS platform, which is something that could be deducted by looking at the product name.

The second section is the **Vector Data**, it contains masks that can be linked to the data ad used to do some further analysis, like computing chl-a by masking the land in order to have the computation only on water.

The third section is the **Tie-point Grids**, these

Name	Type
HDFEOSVersion	ascii
HDFEOS_FractionalOffset_10^nscreans_MODIS_SWATH_Type_L1B	float32
Number_of_Scans	int32
Number_of_Day_mode_scans	int32
Number_of_Night_mode_scans	int32
Incomplete_Scans	int32
Max_Earth_View_Frames	int32
Bit_QA_Flags_Change	int32
Reflective_LUT_Serial_Number_and_Date_of_Last_Change	ascii
Emissive_LUT_Serial_Number_and_Date_of_Last_Change	ascii
QA_LUT_Serial_Number_and_Date_of_Last_Change	ascii
Focal_Plane_Set_Point_State	int8
Doors_and_Screens_Configuration	int8
Earth-Sun_Distance	float32
identifier_product_doi	ascii
identifier_product_doi_authority	ascii
History	Direct read of HDF4 file through CDM library; HDF-EOS StructMetadata
HDF4_Version	4.2.10 (HDF Version 4.2 Release 10, February 7, 2014)
featureType	SWATH
Product_Name	MYD021KM.A2019236.1220.006.2019238185820.hdf
DayNightFlag	Day
Geolocation_File	MYD03.A2019236.1220.006.2019238162511.hdf
Start_Time	2019-08-24 12:20:00.000000
End_Time	2019-08-24 12:25:00.000000
MODIS_Resolution	1km
MODIS_Platform	Aqua

Figure 1: global attribute window

are not data acquired by the sensors in fact, there are ancillary data that are used to support the product. Specifically here are stored information about each pixel of the image like the height, latitude, longitude, solar and sensor Zenith, solar and sensor Azimuth and the Range.

In the last section, called **Bands**, instead, all data are contained, i.e the bands, that are differentiated into two sections. The first one is the **RefSB** (Reflective Solar Band), is the reflection measured by the satellite of the solar radiation, and if it is 100% it means that the whole solar radiation is reflected and if it is less than 100 it means that is partially absorbed. It contains 22 bands where 7 of them have a spatial resolution of either 250 or 500 meters that has been down-scaled to 1 km. The second band section is the **EMISSIVE** containing the emitted bands. Here the bands go from MIR (3750 nm) to TIR (14235 nm). For each of RefSB and EMISSIVE bands in brackets is reported the central channel wavelength. Below are reported two images, one in the red color band (645 nm) and the 31 TIR channel bandwidth (this is usually used because it is almost transparent bandwidth).



Figure 2: RefSB 1 (645 nm)

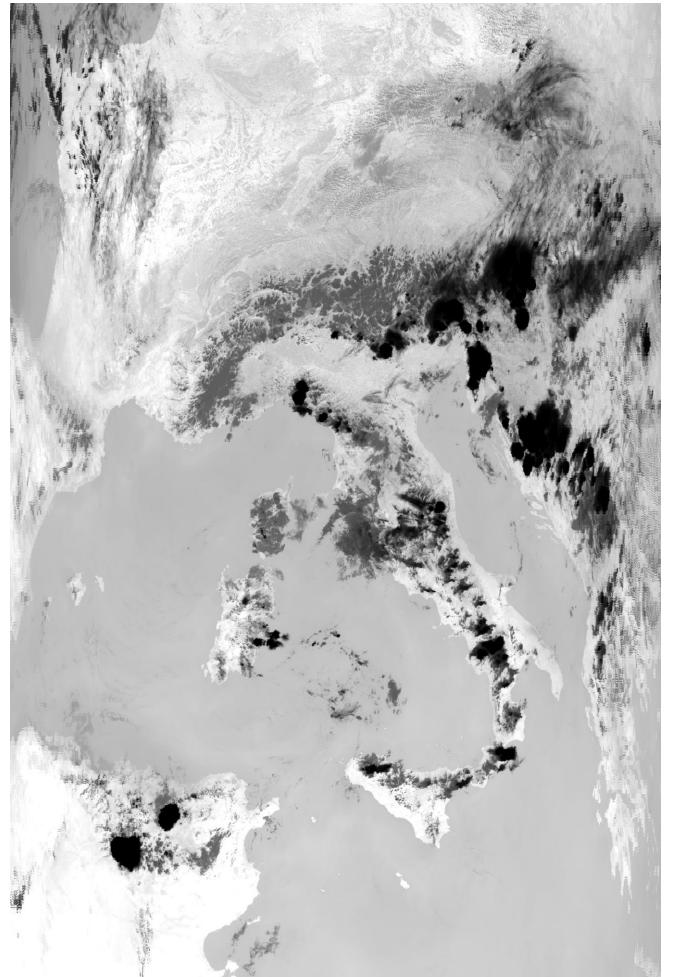


Figure 3: Emissive 31 (11030 nm)

Figure 4 shows the RGB image composite computed by using, for **red**, the **EV_250_Aggr1km_RefSB_1** which corresponds to the central red band (620–670 nm), for **green**, the **EV_500_Aggr1km_RefSB_4** which corresponds to the central green band (545–565 nm) and, for **blue**, the **EV_500_Aggr1km_RefSB_3** which corresponds to the central blue band (459–479 nm).

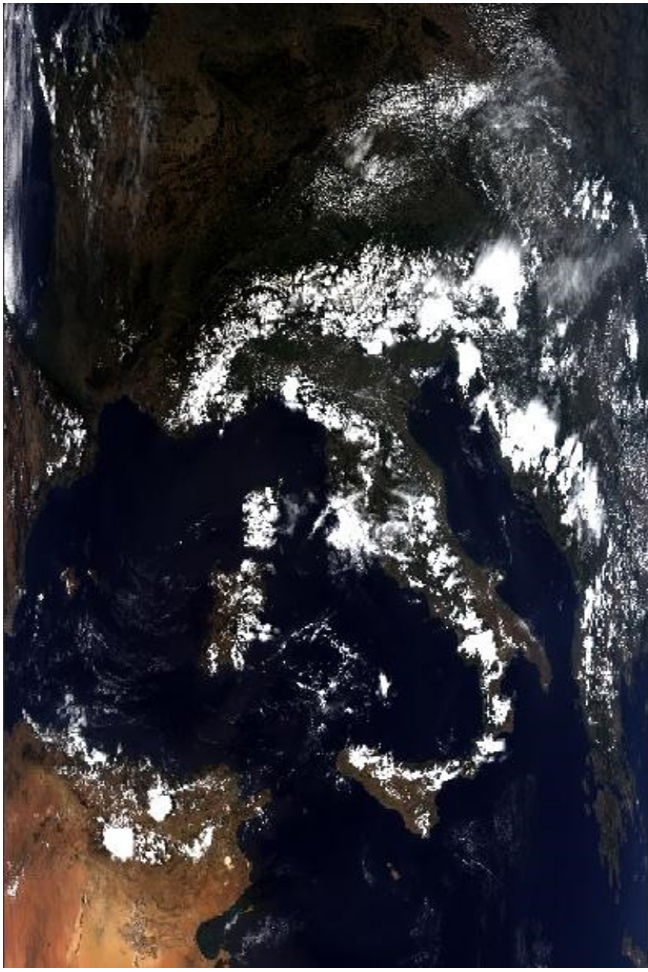


Figure 4: RGB Image

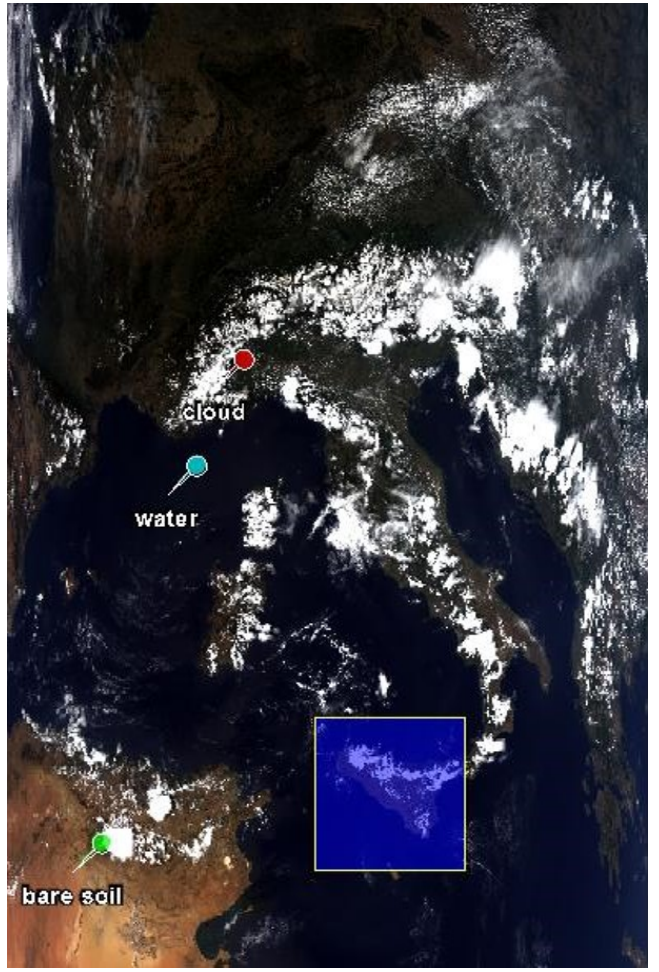


Figure 5: pinned pixels and ROI RGB

3 Perform and display data analysis by spectrum, histogram and profile tools.

The spectrum analysis can be used to analyze the spectra of a selected pixel in the image. In particular it is useful to show how every pixel behaves in different spectral bands. Due to the fact that the **Spectral View tool** works with pixels, the **pin Placing tool** has been used to select 3 points. More precisely, the three selected point represent respectively cloud, water and bare soil pixels, as shown in Figure 5. By looking at the *Reflectance Spectrum View* image below, it is possible to see the spectra behaviour of every pixels for all the reflectance bands provided by the MODIS product. As Figure 6 shows, water has low reflectance, with the highest reflectance value in the blue part of the visible spectrum, whereas it has almost no reflectance in NIR wavelength range. On the other hand, bare soil has a higher reflectance respect to the water, in particular, it has a greater reflectance in NIR. This is due to the fact that there are many factors that actually affect the bare soil reflectance such as soil texture (sand and clay), iron oxide and organic matter. Lastly, the pixel representing cloud shows how it has the picks (i.e. the larger amount of reflected solar radiation) in the blue band. The reflectance (or Albedo) is affected by different factors such as the total mass of water present in the clouds, droplets sizes and shapes and their aggregation and distribution in the cloud space.

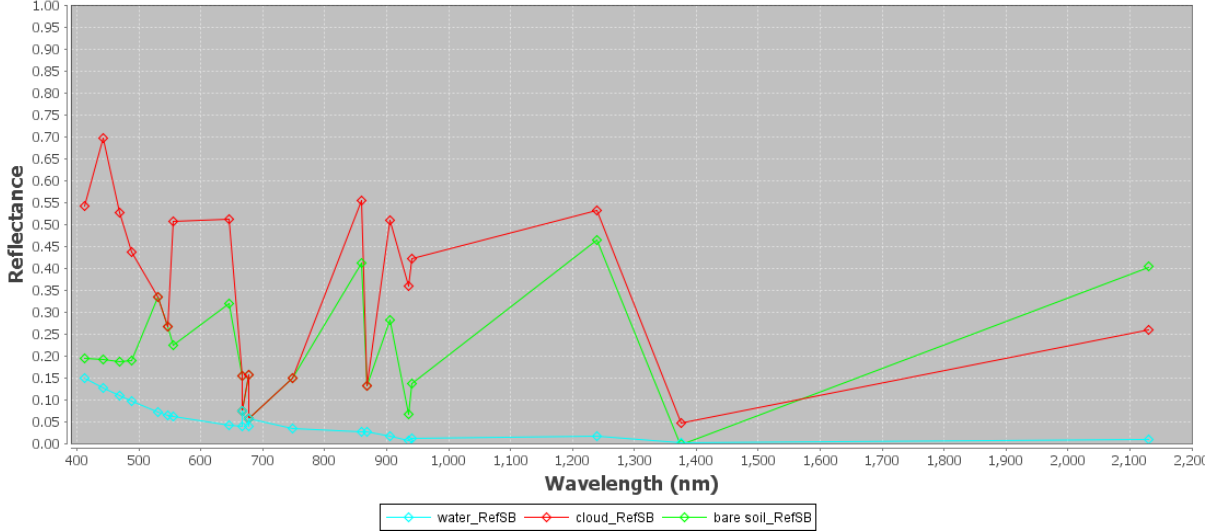


Figure 6: Reflectance Spectrum View

On the other hand, another data analysis on the product can be performed by using the **Histogram Tool** that allows to see pixel distribution on a pre-selected band. Moreover, it is also possible to draw a mask (polygon) in order to exclude all pixels that do not fall in it. In fact, the histogram, represented in Figure 7, shows the pixel distribution, for the 31 TIR channel, in the region of Sicily (the ROI mask is shown in Figure 5). As can be see from the histogram, the pixel distribution is concentrated around an emissivity value of 9 (the most frequent value), and this is reasonable because most of the pixels in the ROI represents water.

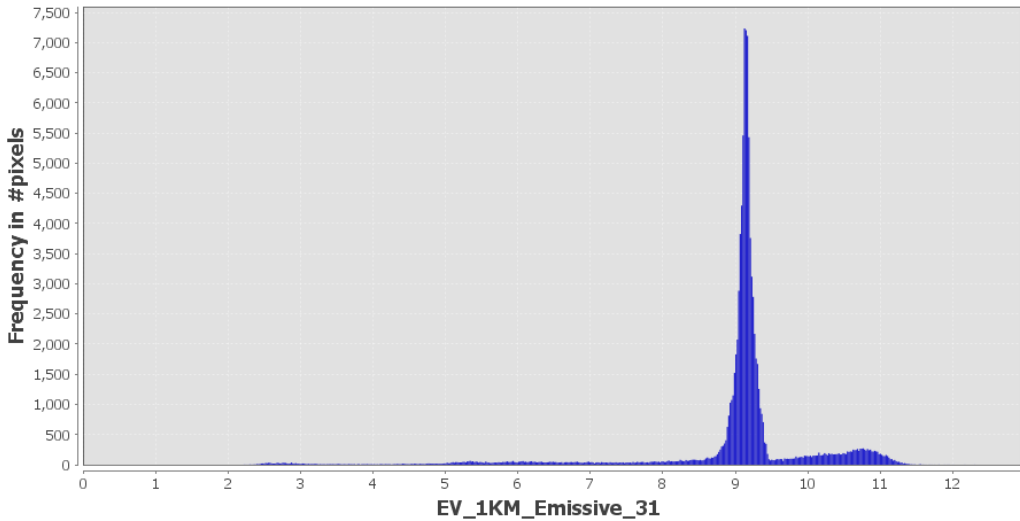


Figure 7: Histogram for EV_1KM_Emissive_31

By using the **Profile Plot tool** it is possible to observe the current emissive value for every pixel. Figure 8 shows the profile plot in the predefined Sicily ROI. The x-axis represents the path length, i.e it shows that there are roughly 1290 pixel values, whereas the y-axis represents the Emissive 31 ($\lambda = 11030\text{nm}$) band. The shaded areas around the line identify the standard deviation of the selected band pixel within a square box (where the square box edge length has been set equal to 5).

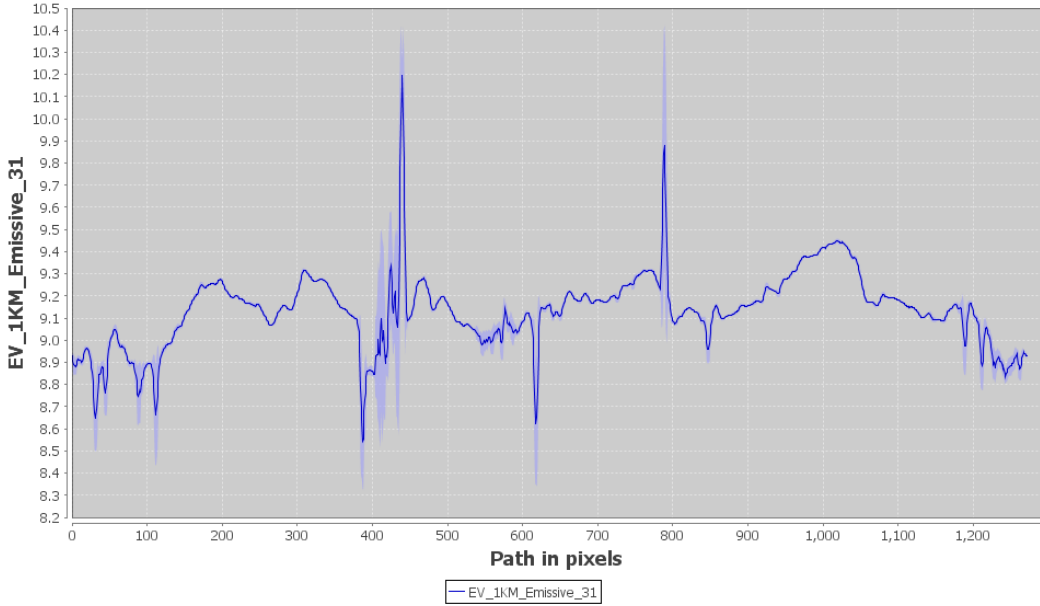


Figure 8: Profile Plot for EV_1KM_Emissive_31

4 Perform and display channel data correlation of the whole image.

Channel data correlation can be performed by plotting 2 different channels in order to see if there is a correlation or not. For that reason, two different channels have been used, a reflectance channel and an emissivity channel. In particular, a red color band with central wavelength at 645 nm and TIR infrared channel centered at 11030 nm, have been chosen. The result is represented by the figure 9. As can be seen from the scatter plot, there is actually not a correlation of the 2 channels, and this is reasonable because they represent the reflection in the red and the emission in TIR, so two different and independent information. On the other hand, if two close channels are plotted together, like the 31 and 32 emissivity channels, then it is possible to see a strong positive correlation (Figure 10).

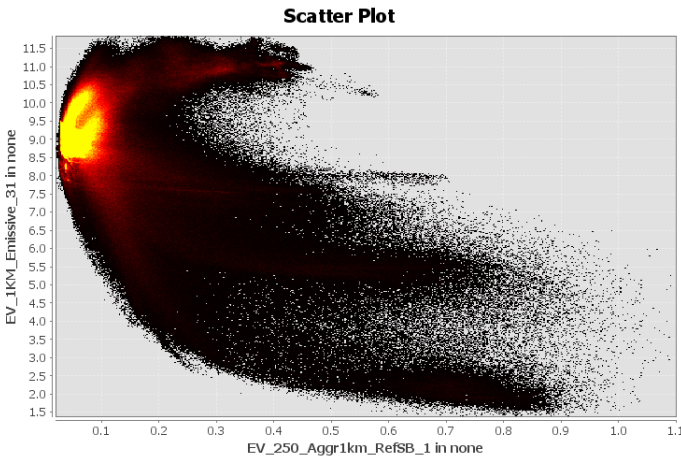


Figure 9: Scatter plot: RefSB 1 and Emissive 31

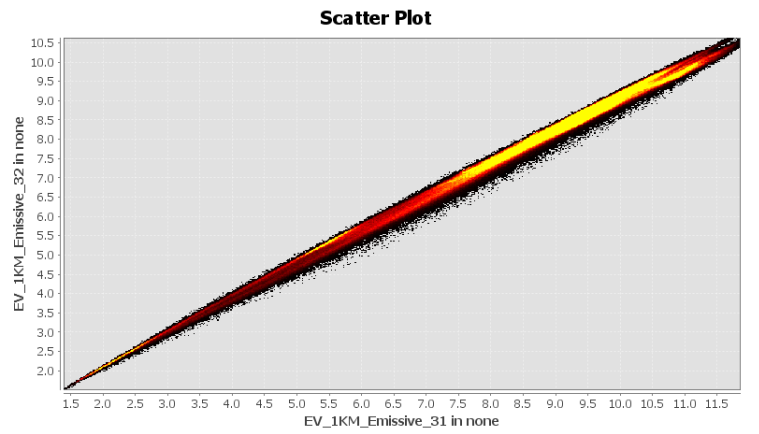


Figure 10: Scatter plot: Emissive 31 and Emissive 32

5 Perform and display channel data correlation of selected ROI (Region of Interest).

Data Correlation can be performed not only on the whole image, but also on a fraction of it. In this way, what is computed is the correlation among channels but only on the pixels belonging to the selected ROI (Region of Interest). A ROI can be selected by using either the **Rectangle drawing tool** or the **Polygon drawing tool**. In this case the **Rectangle drawing tool** has been used to draw a rectangle capturing almost the whole Sardinia island and a fraction of the Tyrrhenian Sea as shown by the false color image (Figure 11). As can be seen from Figures 12 and 13, if two different channels, in particular a red color channel with central wavelength at 645 nm and TIR infrared channel centered at 11030 nm, are plotted together it is possible to see an uncorrelation among them as seen before. This is due to the fact they are bringing highly uncorrelated information. Whereas, if two consecutive channels are plotted together is possible to see a strong positive correlation among them. Of course what is different from the correlations shown before is the amount of pixels that have been considered; here in fact, only a small fraction has been taken in consideration and this can be seen from the plot that presents much less datapoints.

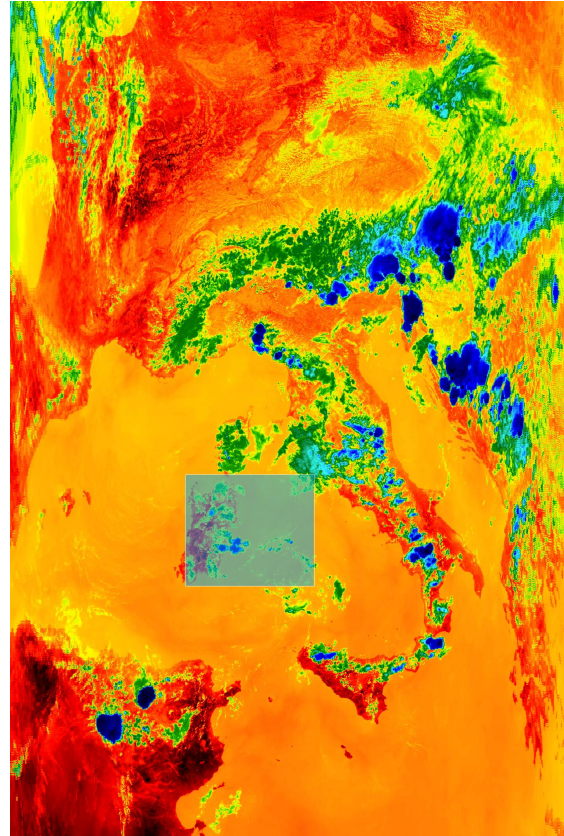


Figure 11: False Color image and selected ROI

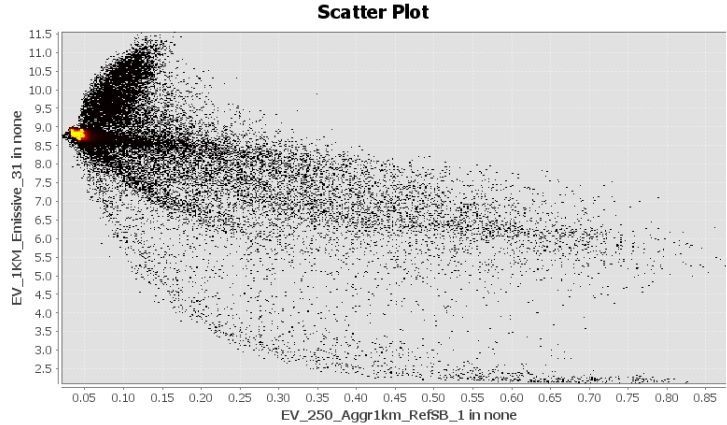


Figure 12: Scatter plot ROI: RefSB 1 and Emissive 31

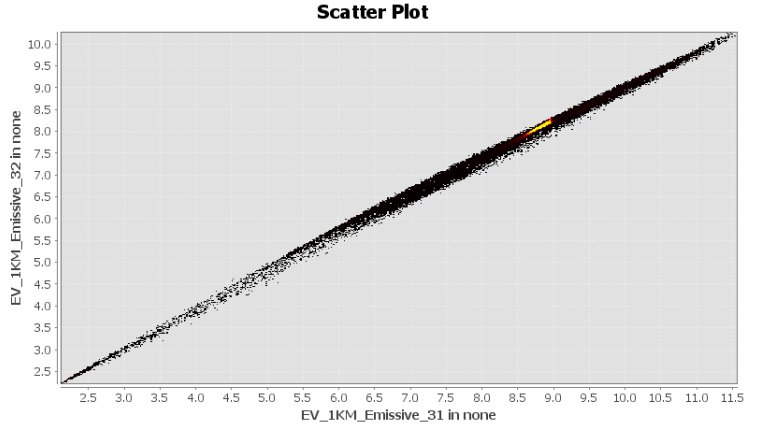


Figure 13: Scatter plot ROI: Emissive 31 and Emissive 31

6 Perform and display principal component analysis

Principal-component analysis, or PCA, is a technique that takes a dataset composed by a set of tuples, representing points in a high-dimensional space, and finds the directions along which the tuples line up best. The set of tuples are handled as a matrix M from which the eigenvectors are returned. The matrix of these eigenvectors can be thought of as a rigid rotation in a high dimensional space. The x-axis corresponds to the principal eigenvector (PC1), the one along which the points are most “spread out”; i.e it is the axis along which the variance of the data is maximized. Likewise, the y-axis corresponds to the second eigenvector (PC2), the eigenvector corresponding to the second-largest eigenvalue. It is the axis along which the variance of distances from the first axis is greatest.

So, with PCA the high-dimensional data are projected into the most important axes (the one with the largest eigenvalues).

In SNAP there are two kinds of implementation for PCA, one can be found under the path: RASTER/IMAGE ANALYSIS, and another one can be found under the **graph builder** operator, as a pipeline brick. Due to the lack of online information and the absolute absence of an official documentation about the implementation in SNAP, it has been decided to use the **Principal Component Analysis** operator, reachable under the path highlighted before, because it returns not only the Principal Components but also:

- **flags:** containing flags masking the pixels included into a pre-chosen ROI.
- **error:** The membership error for a sample. The error is computed by projecting the sample into eigenspace then projecting it back into sample space
- **response:** The dot product of each basis vector against the sample. Can be used as a measure for membership in the training sample set. High values correspond to a better fit.

(See [Principle component Analysis in SNAP](#) for further clarifications).

The **Principal Component Analysis** operator specifies also the correspondence among the principal component and the corresponding band, allowing comparisons among bands. For example, at the end of the process, the first principal component is the one, referred to the band **EV_1KM_RefSB_8**, with a central band set equal to 412nm and the second principal component, referred to the band **EV_1KM_RefSB_9**, with a central of 443nm.

At the end of the process, 38 components have been returned. Figures 14 and 15 show two images, one using principal component 1 and another using principal component 2.

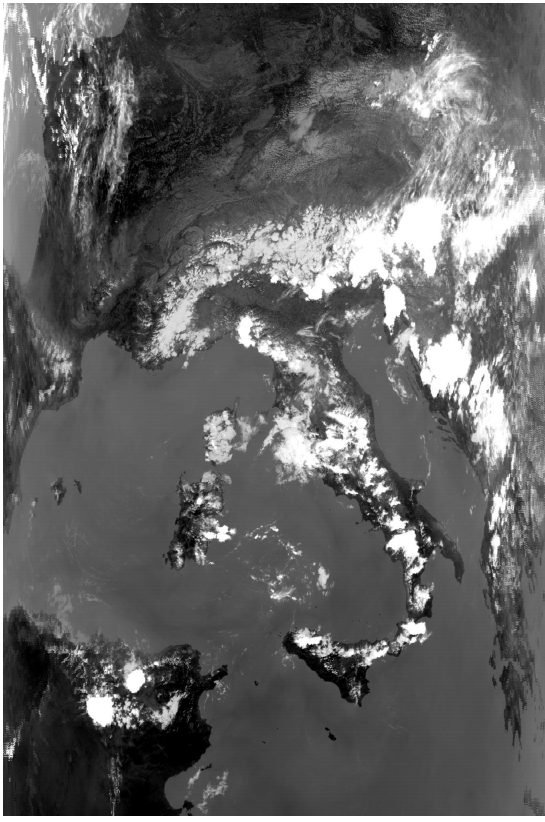


Figure 14: Image with PC 1

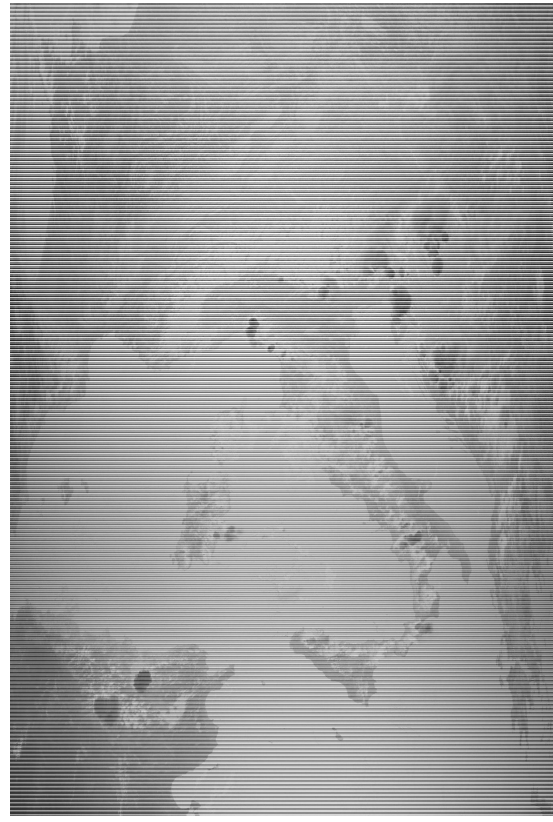


Figure 15: Image with PC 2

By plotting the two channels, the ones with the highest eigenvalues, it is possible to see how the data are projected into an high-dimensional space where line up better and are more spread out. Figure 16 shows the correlation among **EV_1KM_RefSB_8** and **EV_1KM_RefSB_9**, whereas the next shows the PC 1 (referring to the **EV_1KM_RefSB_8** band) and the PC 2 (referring to the **EV_1KM_RefSB_9** band) after Principal component analysis.

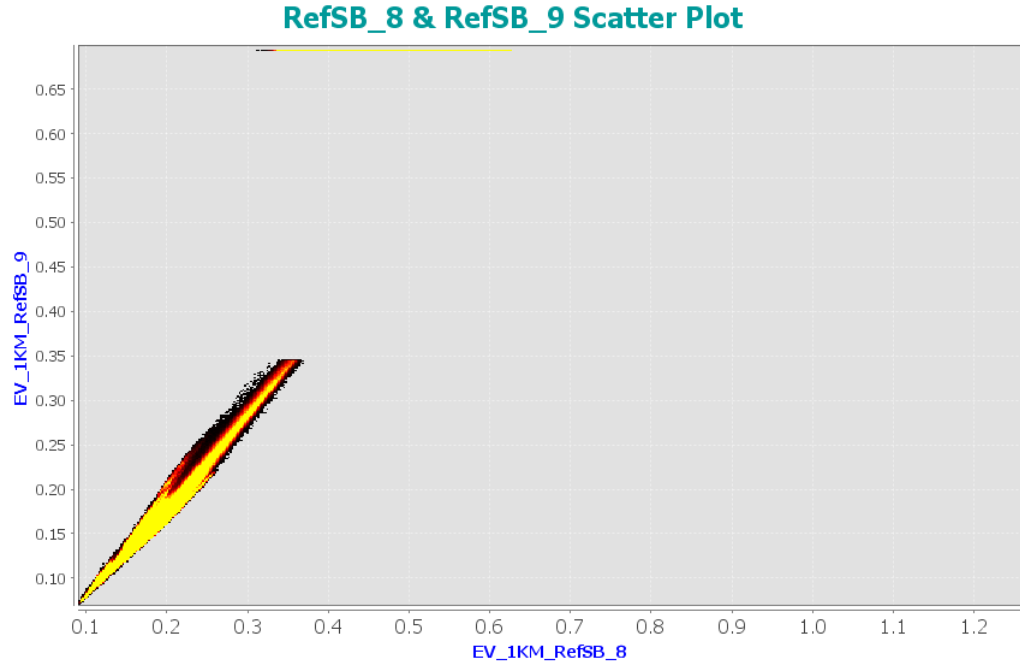


Figure 16: EV_1KM_RefSB_9 and EV_1KM_RefSB_8

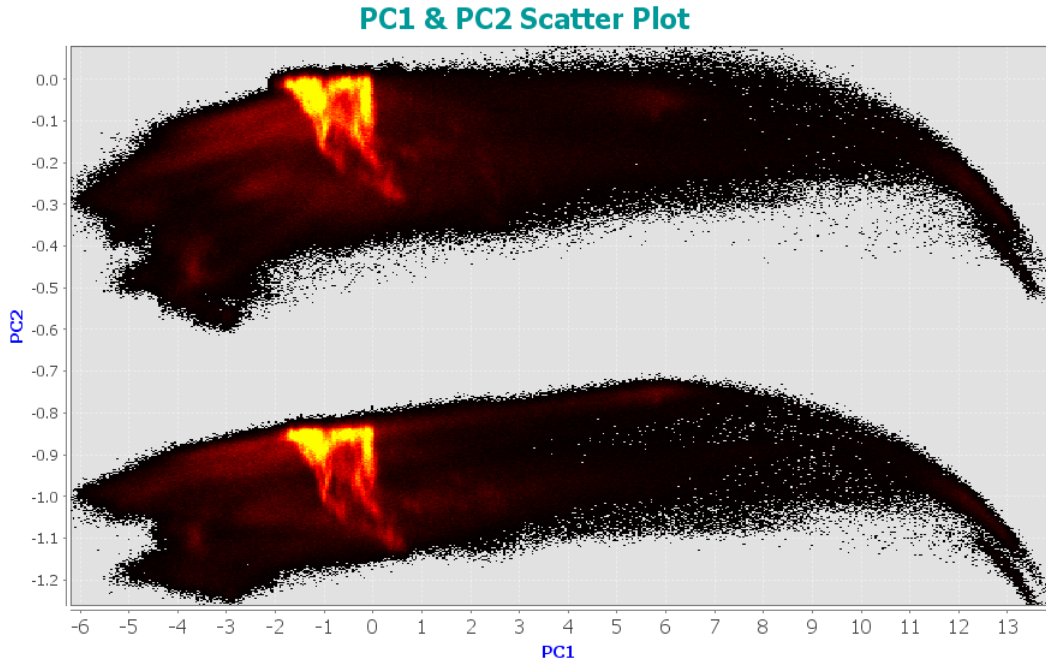


Figure 17: PC1 and PC2

7 Perform, display and interpret unsupervised classification with at least 3 classes (sea, land, cloud)

Due to the fact that in unsupervised classification there is no prior knowledge of what the output should be, here there are not models that require a training part. In particular here, it has been decided to use a cluster analysis, by using k-means algorithm, in order to see how well it is able to group by pixels in same clusters to reproduce the original image. In order to perform cluster analysis, it has been used the **K-Means Cluseter Analysis** operator implemented in SNAP available under the path: RASTER/CLASSIFICATION/UNSUPERVISED CLASSIFICATION. The Algorithm takes in input 3 parameters:

- **N° of clusters:** it has been set equal to 3 in order to detect sea, land and clouds.
- **N° of iterations:** it has been set equal to 100. This parameter is necessary in order to avoid that the centroids' update last forever, because the algorithm stops when a convergence criterion is met; and this could happen either the centroids did not change among two different iterations, or when a given threshold is met (the maximum number of iterations)
- **Random Seed:** it has been set equal to 31415. This is used to replicate the results, because the K-Means Algorithm starts with a pseudo-random distribution of the initial centroids. So, this number is used to initializes this pseudo-random number generator, used to generate the initial clusters (initial centroids).

Whereas, regarding the bands, all of the components returned after the PCA have been used. Figure 18 shows the classification. Blue areas represent waters, yellow regions represent land and white represent clouds.

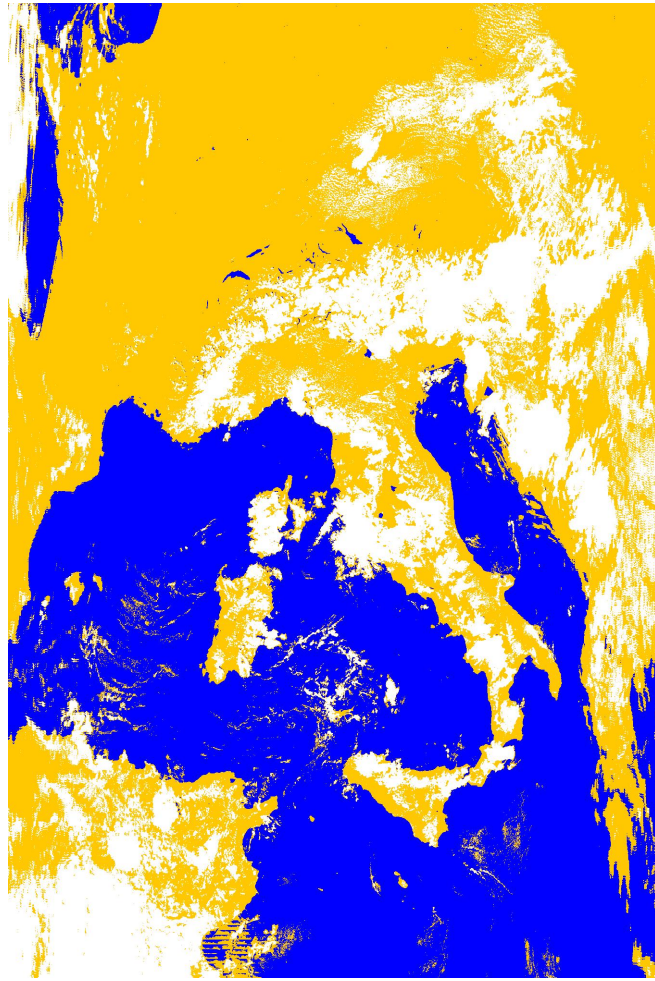


Figure 18: K-Means Cluster Analysis

Comparing this classification with the RGB image (Figure 4), it is possible to see that the algorithm has performed a very accurate classification, even though it returns a higher presence of clouds in the Tunisia country, that is actually untrue, and it also performs some missclassifications nearby Corsica and Sardinia islands, where it classifies some clouds as lands. But, by looking at the overall classification, it is possible to say that the returned results are quite accurate. In fact it is also able to correctly identify Bolzano Trasimeno and Garda lakes in Italy but also many lakes in Central Europe, in particular in Switzerland (like Bodensee, Zürichsee, Vierwaldstättersee, Thunersee, Brienzersee and Lac Léman lakes). Figure 19 shows the classification exported in Google Earth in order to show how k-means performs very well on classifying lakes in Central Europe. The white represents the predicted clouds, the blue the lakes, whereas for the land it has been decided to not use color in order to show real land color. It is necessary to highlight that, in order to export the classification on Google Earth, the product has been reprojected (by using the **Reprojection** operator) in Latitude/Longitude geographical coordinates.

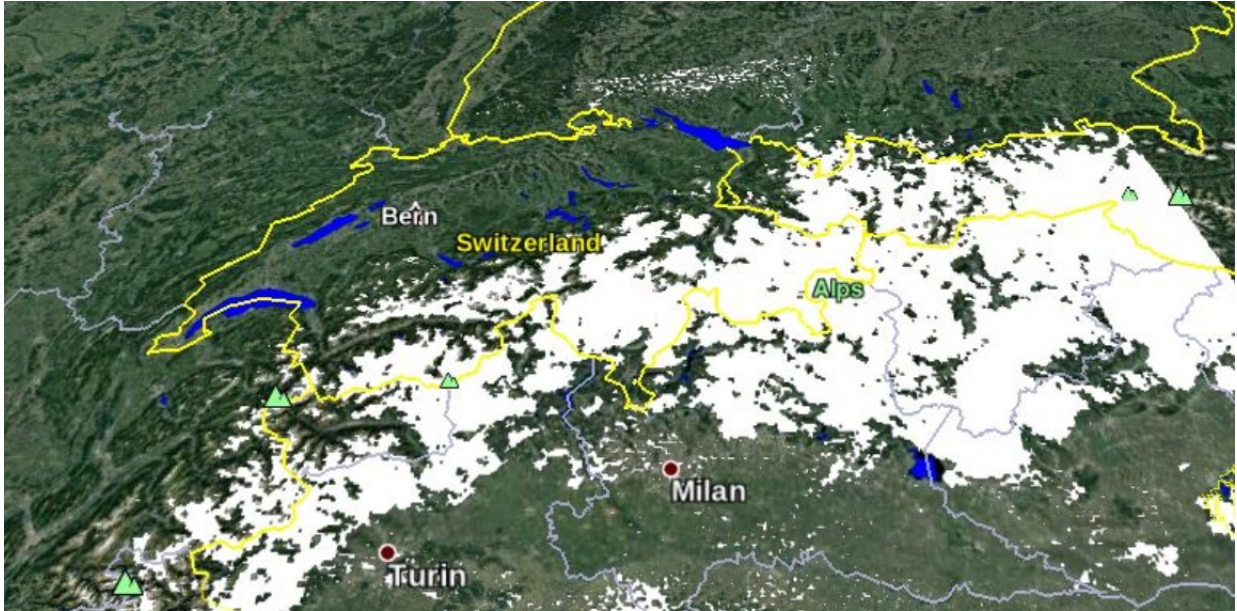


Figure 19: K-Means Cluster Analysis

8 Perform, display and interpret supervised classification with at least 4 classes (sea, land, cloud)

When a supervised classification has to be performed, what is necessary is to train a predictive model on training data and than use it on unseen data to perform classification. In order to create train data in SNAP, as first step is necessary to create some sort of containers called **Vector Data Container**(reachable under the vector section in SNAP). Once the vector containers have been defined it is necessary to assign them data (pixels), and this can be accomplished by drawing polygons on the image. Figure 20 shows all the polygons used to fill up the 4 vector containers. Per each container 3 polygons have been realized on the image that can be distinguished by the colors. Every color represent a different vector container: purple = land, yellow = clouds, fuchsia = water, aqua green == bare soil/unvegetated areas. The image represents comes from the plot of the first principal component.

Once the vectors have been filled up with data, the **Random Forest Classifier** has been trained on them. Random Forest Algorithm implemented in SNAP allows to set different parameters, in particular: *number of training samples* has been set equal to 10000, *the number of trees* has been set equal to 50 and for *feature bands* all the principal components has been used. Moreover, at this stage, only 3 classes have been used: water, clouds and land, in order to see how well the classifier was able to perform. Figure 21 shows the results after running the Random Forest Classifier.

As can be seen from Figure 21, Random Forest Classifier (RFC) performs quite well on classification, in particular regarding cloud detection. However, as it shown on the figure, there are some black areas representing pixels that have not been assigned to a class due to the lack of information. In particular, since their associated reflectances did not allow to, based on the trained model, associate them to a well known class, they have been marked in black. The RFC actually performed also some misclassifications while detecting clouds in the Mediterranean Sea, where it confuses clouds with lands; but probably this is not a missclassification but it could depend on the fact that clouds are carrying sand particles coming from the North Africa desert. So, in order to increase the performances of the Algorithm and also try to better investigate this sand phenomena, it has been decided to work with one more class, four in total. The forth class is the one referred to the bare soil/unvegetated areas. Also here, the RFC, with the same settings, has been executed but with 4 classes instead of 3. Figure 22 shows the results.

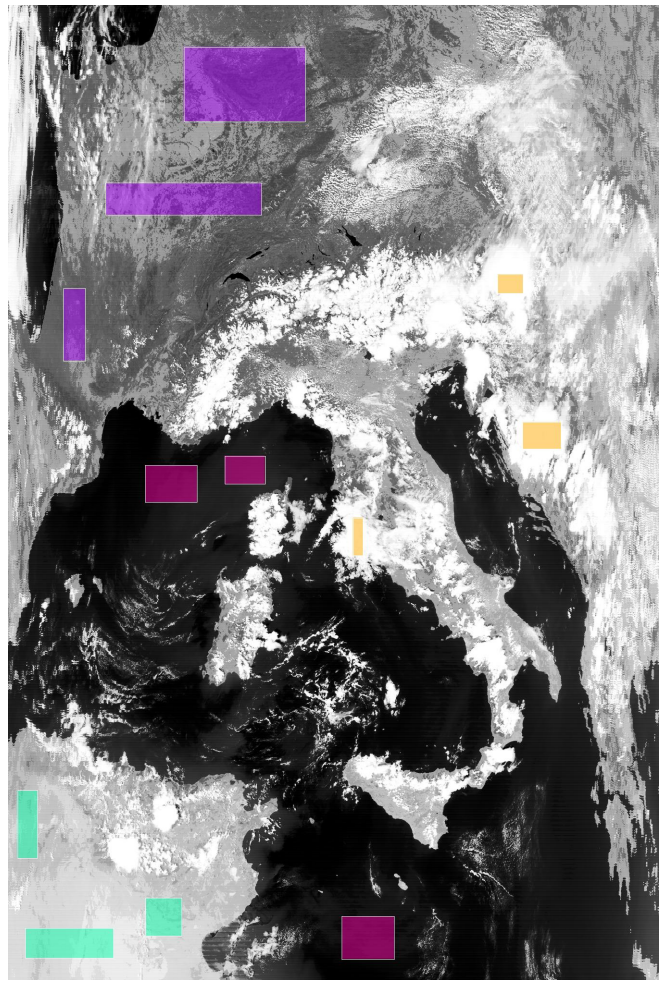


Figure 20: Vector data and assigned polygons

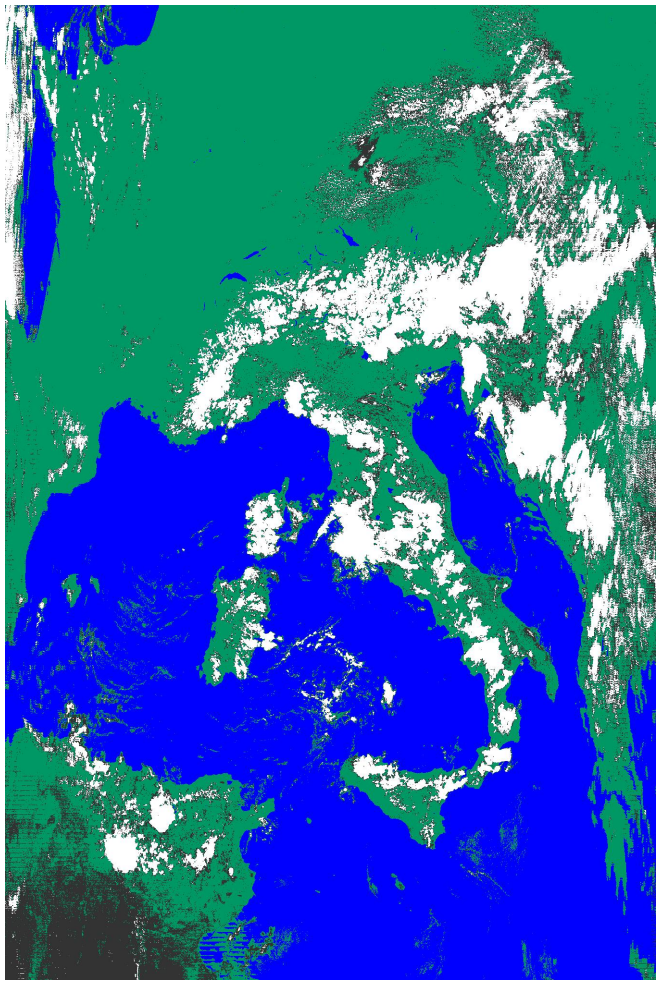


Figure 21: Three classes classification by Random Forest Classifier

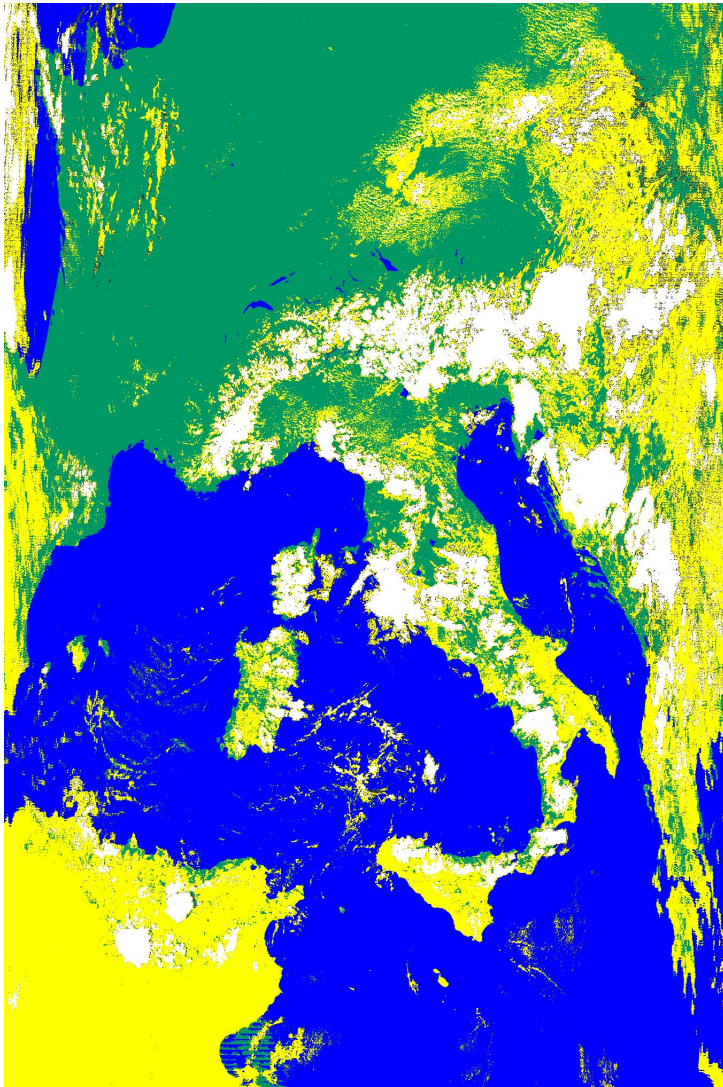


Figure 22: Four classes classification by Random Forest Classifier

As can be seen from figure 22, there are still some unclassified areas (black pixels), but the overall quality of the classification seems to be highly improved. In particular, recalling the previous assumption about the sand in clouds, by performing these four classes classification (using as training data for the 4th class data coming from the Tunisia desert) it seems that the assumption could actually be real. Of course this is still an assumption and a further analysis should be performed in order to be sure, but it might be a good starting point. Moreover, by using one more class, it is possible to distinguish also some urban areas around big cities like Rome, Florance and Emilia Romagna region (Bologna, Modena, Ferrara, Padova and Forlì cities). This can be highlighted by exporting this classification in Google Earth. As done during section 7, before exporting the the Classification in Google Earth, the product has been resampled around Italy an reprojected in Lat/Long geographical coordinates. The exportation is shown in figure 23.



Figure 23: Four classes classification around Italy on Google Earth

9 Implement at least 3 formulas of 2-band and 3-band vegetation index (VI) using SNAP processing tools

In literature, many different indexes have been defined in order to estimate and evaluate vegetation characteristics. Here, what it has been decided to exploit are some mathematical combinations of visible and NIR reflectance bands present in MODIS products. These indexes can be used for many purposes like seeing the conditions and the changing of the vegetation either during different periods or to detect deforestation actions in crucial areas, and so on. In this particular case they have been used to stress most vegetated areas and see how the vegetation changes during winter and summer.

For this task, five different vegetation indexes have been computed by using **Band Maths** processing tool implemented in SNAP. Below have been reported the formula of the different calculated indexes:

$$NDVI = \frac{\rho_{NIR} - \rho_{Red}}{\rho_{NIR} + \rho_{Red}} \quad (1)$$

$$SR = \frac{\rho_{NIR}}{\rho_{Red}} \quad (4)$$

$$EVI = 2.5 \frac{\rho_{NIR} - \rho_{Red}}{1 + \rho_{NIR} + 6\rho_{Red} - 7.5\rho_{Blue}} \quad (2)$$

$$CI_Green = \frac{\rho_{NIR}}{\rho_{Green}} - 1 \quad (5)$$

$$GARI = \frac{\rho_{NIR} - [\rho_{Green} - \gamma(\rho_{Blue} - \rho_{Red})]}{\rho_{NIR} + [\rho_{Green} - \gamma(\rho_{Blue} - \rho_{Red})]} \quad (3)$$

These indexes have been calculated by using the reflectance bands present in MODIS product. In particular:

- **red**: the central band of 620–670 nm
- **green**: the central band of 545–565 nm
- **blue**: the central band of 459–479 nm
- **NIR**: the central band of 841–876 nm

The **NDVI** (Normalized Difference Vegetation Index) is one of the best indicator of healthy vegetation. It is a robust index and can be used in different kind of conditions, due to the fact that it combines the peculiarity of the computation of its normalized difference and the use of the highest absorption and reflectance regions of chlorophyll. The index spans from values between -1 and 1; lower values identify unhealthy vegetation, whereas values close to 1 represent healthy vegetation (green) [5].

The **SR** (Simple Ratio) Index is a ratio of the highest reflectance wavelength for vegetation and the deepest chlorophyll absorption wavelength. As for NDVI, it is effective over a wide range of conditions and it can saturate in dense vegetation when LAI (Leaf Area Index) becomes very high [2].

The **EVI** (Enhanced Vegetation Index) index has been developed as an improvement of the well known NDVI that may saturate in areas with high LAI. It uses the blue reflectance region to correct for soil background signals and to reduce atmospheric influences, including aerosol scattering. It spans from 0 to 1 [1].

The **CI_Green** (Green Chlorophyll Index) is used to estimate leaf chlorophyll content across a wide range of plant species. Due to the fact it works with NIR and green wavelength, it provides a better prediction of chlorophyll content while allowing for more sensitivity and higher signal-to-noise ratio [3].

The **GARI** (Green Atmospherically Resistant Index) is an index which is more sensitive to a wide range of chlorophyll concentrations and less sensitive to atmospheric effects than NDVI. The γ constant is a weighting function that depends on aerosol conditions in the atmosphere. A value of 1.7 is recommended [4].

10 Apply at least 3 VI formulas to land pixels and interpret their output results and differences

By using the **Band Maths** operator, the five formulas have been applied on the product and the five pictures below show the results:

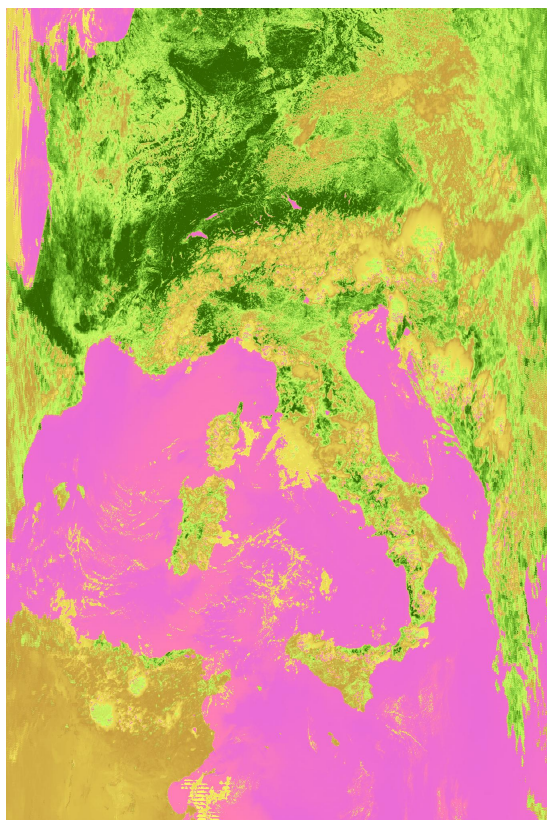


Figure 24: NDVI Vegetation Index

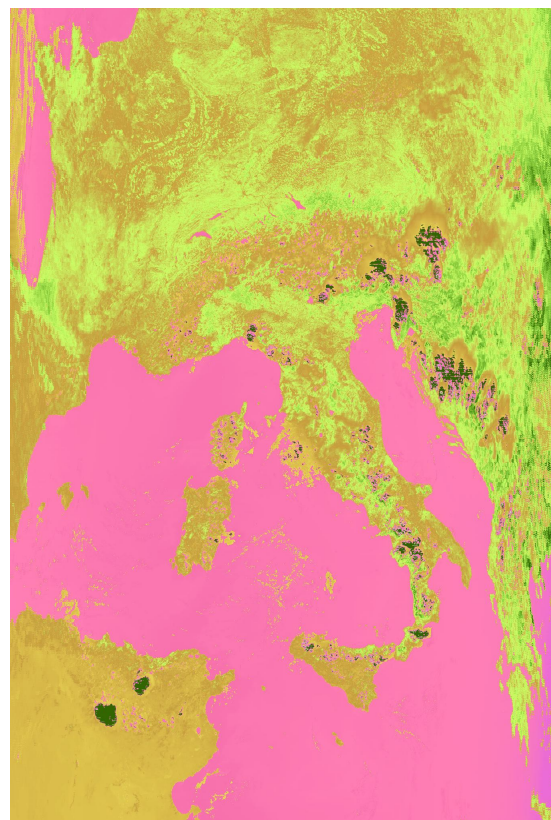


Figure 25: EVI Vegetation Index

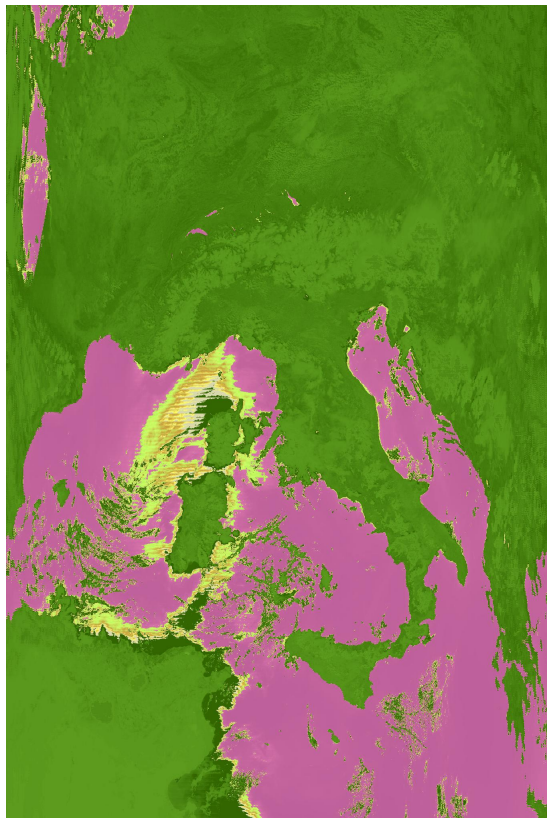


Figure 26: GARI Vegetation Index

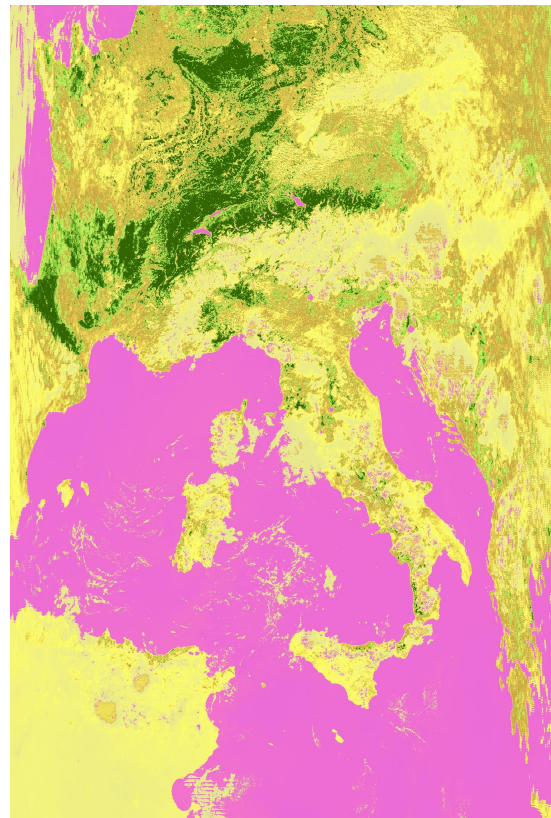


Figure 27: SR Vegetation Index

As can be seen from the results shown in Figures from 24 to 28, different indexes perform differently and some seems to have higher performances than others. In fact, the NDVI VI is the one performing better to identify targets containing healthy vegetation. In fact, it highlights dense vegetation canopies by assigning to these pixels very high values, from 0.4 to 1. Moreover, due to the fact that water has a very low reflectance in both used spectral bands (NIR and Red), it assigns to them very low positive values (even though this cannot be shown because water pixels areas have been masked out, as required.). Also soil areas can be identified because they have a very low positive NDVI values (among 0.1 and 0.2) due to the fact that these areas have a NIR spectral reflectance larger than in the Red band. In addition, the index can easily distinguish clouds, since they have a very low reflectance in both bands. The computed NDVI VI for these pixels tends to very negative values, in fact the false color representation shows them with a yellowish color. However, this is true for big and dense clouds, whereas for thin/small clouds and clouds shadows can actually mislead the index. For that reason, in order to reduce this effect, composite images coming from daily images are composed.

The EVI VI instead, is an index optimized to enhance the vegetation signal in high biomass areas thanks to the fact that it tries to reduce the atmosphere influences. Differently from the NDVI, the EVI VI is more reactive to canopy variations, canopy type, plant physiognomy, and canopy architecture. In fact, these two indexes are complement and can be combined to increase the quality of the analysis in vegetation changes.

The GARI VI on the other hand, does not perform very well in fact, almost the entire areas are represented in green. The CI_Green VI instead performs similarly to the NDVI VI, due to the fact that both work with NIR bands.

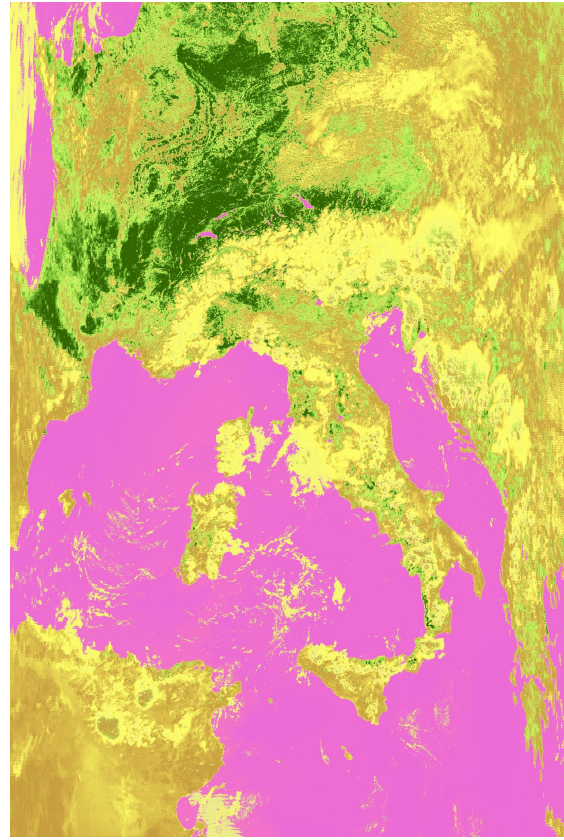


Figure 28: CI_Green Vegetation Index

11 Perform an unsupervised classification by using an arbitrary VI index instead of MODIS channel

As described in the previous section, for this product, the most reliable Vegetation Index seems to be the NDVI. For that reason, in this section, it has been tested the capability of the unsupervised k-means Algorithm to perform a 3 class classification by using the NDVI index instead of included MODIS channel bands. Figure 29 shows the returned classification.

The returned classification seems to be quite faithful to the original one (Figure 4) when it classifies lands and waters; whereas, when it classifies clouds it performs misclassifications in particular around the Tunisia area. Of course this is reasonable because this area is mostly covered by desert and bare soil, areas with low positive NDVI values (around 0.1).

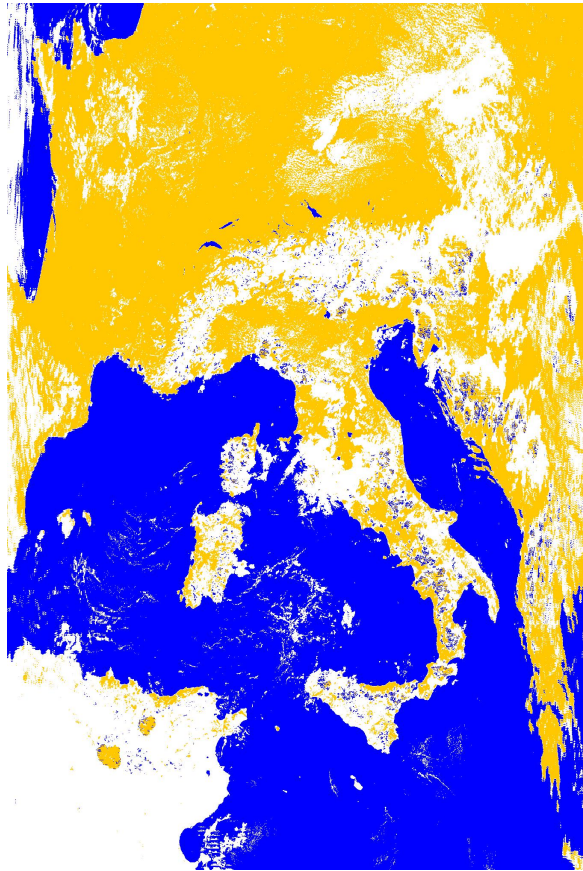


Figure 29: Three classes classification by using NDVI VI

12 Download a second MODIS image at 1-km resolution over the same geographical area of interest during a winter season. Apply the same selected VI index and qualitatively compare the differences.

By looking at the [NASA LAADS DAAC database](#), a second image with same target area has been downloaded but in this case the acquisition is referred to the winter period, in particular the acquisition date back to December 27 of 2018. The referring product is the following one

MYD021KM.A2018361.1220.006.2018362150602.hdf where:

- **Product Short name:** MYD021KM, where *MYD* stands for Aqua platform, *02* stands for calibrated product, *1KM* is the spatial resolution
- **Julian Date of Acquisition:** A2018361, *A* stands for acquisition and *361* is the 361th day
- **Hours and Minutes of Acquisition:** 1220
- **Collection Version:** 006
- **Julian Date of Production:** 2018362150602
- **Data Format:** hdf

Taking a look at the specifications of the product, it is possible to see that the acquisition hour is exactly the same as for the summer acquisition. Moreover, it is also reported that there are not incomplete scans acquisitions, meaning that there are not uncovered areas. Also on this product, the most reliable VI, among the ones applied on the summer acquisition, has been also computed, by using the **Band Maths** operator. Figure 30 shows the RGB composite image (using the **EV_250_Aggr1km_RefSB_1**,

EV_500_Aggr1km_RefSB_4 and **EV_500_Aggr1km_RefSB_3** bands) and figure 31 shows the NDVI VI on the winter product:

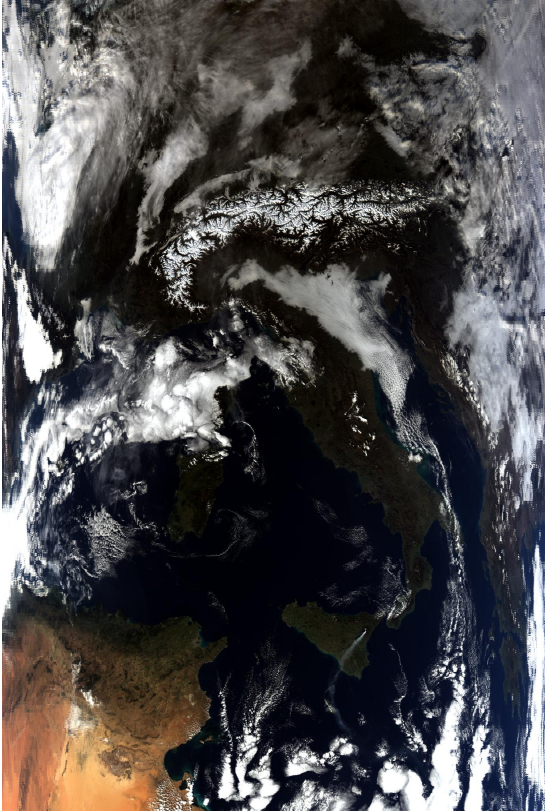


Figure 30: RGB Winter Acquisition

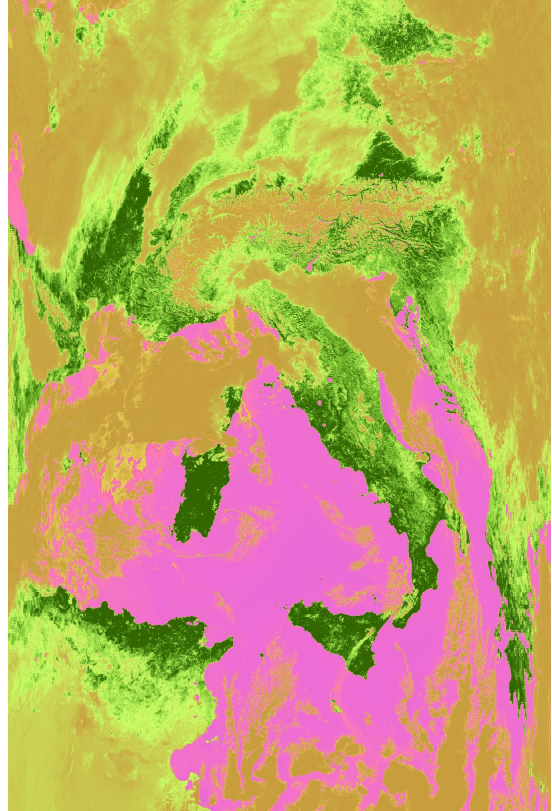


Figure 31: NDVI on Winter Acquisition

As Figure 31 shows, areas that were less vegetated during summer have now a very high NDVI value, in particular, the areas belonging to the north of Tunisia and the two Italian biggest islands. But most in general, the whole Italian Peninsula seems improved in terms of vegetated areas, highlighting how the hot summer of last year reduces the quantity of healthy vegetation all over the territory. The purple color highlights that the NDVI VI has not been applied on water.

13 To perform a quantitative change detection (difference) of the vegetation coverage class by reprojecting the 2 winter and summer MODIS images over the same grid in a selected region of interest (ROI).

In order to better show the differences among winter and summer acquisitions, what has been done was to build up a binary mask to highlight areas with strong NDVI values. More precisely the used binary mask consists of assigning 1 if the NDVI value is ≥ 0.5 and 0 otherwise. The threshold of 0.5 has been chosen because, as we remember, this VI spans from -1 to 1 so, due to the fact the goal is to underline areas with strong changes in healthy vegetation, a so high value has been fixed. Figures below show respectively the NDVI mask for both acquisitions, winter and summer.

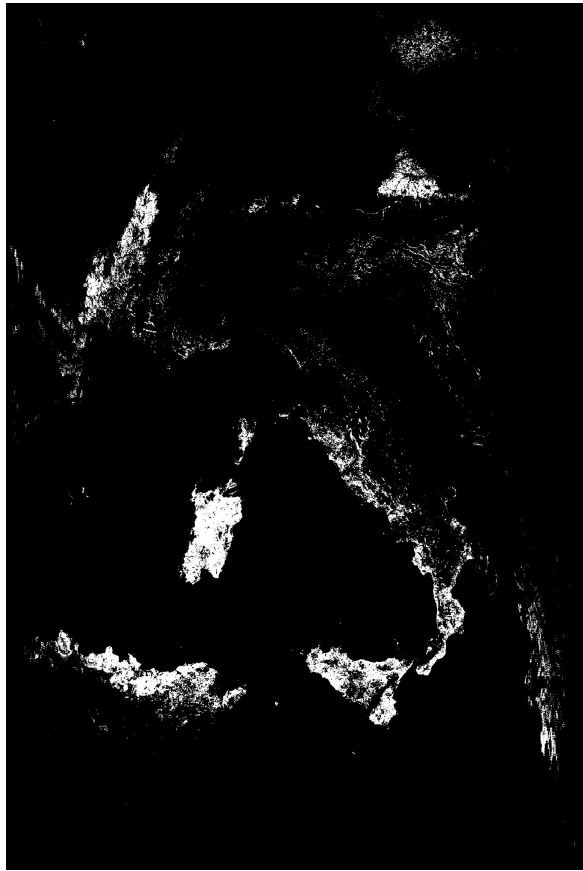


Figure 32: Winter NDVI mask



Figure 33: Summer NDVI mask

Figures 32 and 33 show how vegetated areas change during winter and summer. In particular, areas that are not so highly vegetated during the winter become more vegetated during summer, and the other way around. In fact, areas in south of Italy and north of Africa, that are more exposed to high temperature, are more affected by vegetation level reductions.

References

- [1] Huete A. et al. Overview of the radiometric and biophysical performance of the modis vegetation indices. *Remote Sensing of Environment*, (83):195–213, 2002.
- [2] Birth G. and G. McVey. Measuring the color of growing turf with a reflectance spectrophotometer. *Agronomy Journal*, (60):640–643, 1968.
- [3] Y. Gritz Gitelson A. and M. Merzlyak. Relationships between leaf chlorophyll content and spectral reflectance and algorithms for non-destructive chlorophyll assessment in higher plant leaves. *Journal of Plant Physiology*, (160):271–282, 2002.
- [4] Y. Kaufman Gitelson A. and M. Merzlyak. Use of a green channel in remote sensing of global vegetation from eos-modis. *Remote Sensing of Environment*, (58):289–298, 1996.
- [5] J. Schell Rouse J., R. Haas and D. Deering. Monitoring vegetation systems in the great plains with erts. *Third ERTS Symposium, NASA*, pages 309–317, 1973.